Development/Plasticity/Repair

Prenatal Ethanol Exposure Disrupts Intraneocortical Circuitry, Cortical Gene Expression, and Behavior in a Mouse Model of FASD

Hani El Shawa,* Charles W. Abbott III,* and Kelly J. Huffman
Department of Psychology and Interdepartmental Neuroscience Program, University of California, Riverside, Riverside, California 92521

In utero **ethanol exposure from a mother's consumption of alcoholic beverages impacts brain and cognitive development, creating a range of deficits in the child (Levitt, 1998; Lebel et al., 2012). Children diagnosed with fetal alcohol spectrum disorders (FASD) are often born with facial dysmorphology and may exhibit cognitive, behavioral, and motor deficits from ethanol-related neurobiological damage in early development. Prenatal ethanol exposure (PrEE) is the number one cause of preventable mental and intellectual dysfunction globally, therefore the neurobiological underpinnings warrant systematic research. We document novel anatomical and gene expression abnormalities in the neocortex of newborn mice exposed to ethanol *in utero*. This is the first study to demonstrate large-scale changes in intraneocortical connections and disruption of normal patterns of neocortical gene expression in any prenatal ethanol exposure animal model. Neuroanatomical defects and abnormal neocortical *RZRβ*, *Id2*, and *Cadherin8* expression patterns are observed in PrEE newborns, and abnormal behavior is present in 20-d-old PrEE mice. The vast network of neocortical connections is responsible for high-level sensory and motor processing as well as complex cognitive thought and behavior in humans. Disruptions to this network from PrEE-related changes in gene expression may underlie some of the cognitive-behavioral phenotypes observed in children with FASD.**

Introduction

Fetal alcohol spectrum disorders (FASD) describe a continuum of developmental defects in offspring caused by maternal consumption of alcohol during pregnancy (Hoyme et al., 2005). FASD is a classification that includes fetal alcohol syndrome (FAS), partial FAS, fetal alcohol effects, alcohol-related neurodevelopmental disorder, and alcohol-related birth defects (Jones et al., 2010). Children with FASD exhibit physical, cognitive, and behavioral deficits that may include learning disabilities, reduced IQ, facial dysmorphologies, mental retardation, and anxiety/depression (Green, 2007; Jones et al., 2010; Jacobson et al., 2011; Lebel et al., 2012). The pervasive nature of FASD in society has led the World Health Organization to deem prenatal exposure to alcohol the leading preventable cause of mental retardation in Western civilization.

Recent reports indicate that up to 12% of US women drink while pregnant (CDC, 2012; Santiago et al., 2013; Waterman et al., 2013). This estimate is likely an underestimate as new, sometimes anecdotal, literature has infiltrated the media promoting the safety of drinking during pregnancy (Kelly et al., 2009, 2012; Robinson et al., 2010; Skogerbø et al., 2012; Oster, 2013). This literature conflicts with data from developmental biologists and neuroscientists who have outlined the deleterious effects of prenatal ethanol exposure (PrEE) in controlled human and animal studies (Galofré et al., 1987; Bailey et al., 2001; Zhou et al., 2003, 2005; Powrozek and Zhou, 2005; Hoffman et al., 2008; Livy and Elberger, 2008; Tochitani et al., 2010; Zucca and Valenzuela, 2010; Mah et al., 2011; Day et al., 2013).

Developmental disorders are thought to arise from abnormal development of the neocortex, as it regulates complex behavior, cognition, and other high-level processes (Beckmann, 1999; Gillberg, 1999; Courchesne et al., 2005; Dawson et al., 2005; Pardo et al., 2005; Johansson et al., 2006; Pelka et al., 2006). Early gene expression patterns the cortex and regulates the development of intraneocortical connections (INCs) that integrate sensorimotor information and underlie cortical function (Huffman et al., 2004; Dye et al., 2011a,b, 2012). We hypothesize that PrEE alters gene expression, which in turn produces errors in neocortical network development leading to behavioral change in a mouse model of FASD.

As predicted, our results demonstrate a dramatic positional shift of developing INCs where aberrant connections are observed between frontal, somatosensory, and visual cortex in newborn PrEE mice, a previously undiscovered PrEE-induced defect in neocortical organization and network development. Neocortical expression patterns of *RZRβ*, *Id2*, and *Cadherin8*, genes known to play a role in cortical patterning (Huffman et al., 2004; Dye et al., 2011a,b), are also shifted in PrEE mice. The PrEE-

Received Aug. 30, 2013; revised Oct. 22, 2013; accepted Oct. 23, 2013.

Author contributions: K.J.H. designed research; H.E.S., C.W.A., and K.J.H. performed research; H.E.S., C.W.A., and K.J.H. analyzed data; K.J.H. wrote the paper.

This work was supported by the National Institute on Alcohol Abuse and Alcoholism at the National Institutes of Health (1R03AA021545-01 to K.J.H.). We thank Sarah Santiago and Olga Kozanian for technical help with experimental techniques.

The authors declare no competing financial interests.

*H.E.S. and C.W.A. contributed equally to this work.

Correspondence should be addressed to Dr Kelly J. Huffman, Department of Psychology and Interdepartmental Neuroscience Program, University of California, Riverside, 900 University Avenue, Riverside, CA 92521. E-mail: kelly.huffman@ucr.edu.

DOI:10.1523/JNEUROSCI.3721-13.2013

 0270-6474/13/3318893-13$15.00/0

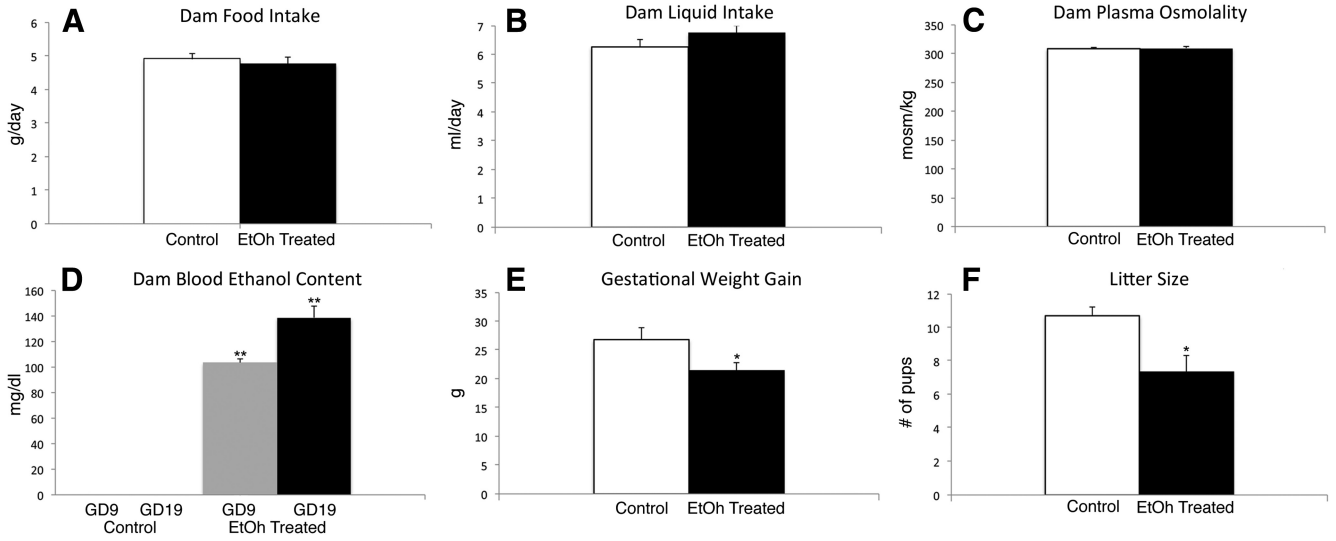

Figure 1. Measurements in ethanol (EtOH)-treated and control dams. Black and gray bars, EtOH-treated dams. White bars, control dams. ***A***, Average dam food intake (g/d). No significant differences (EtOH-treated, $n = 10$; control, $n = 10$). ***B***, Average dam liquid intake (ml/d). No significant differences (EtOH-treated, $n = 10$; control, $n = 10$). ***C***, Average dam plasma osmolality (mosm/kg). No significant differences (EtOH-treated, $n = 7$; control, $n = 5$). ***D***, Average dam blood ethanol content (mg/dl) at GD9 and GD19. EtOH-treated dams (GD9 $n = 6$, GD19 $n = 9$) showed significantly higher BEC levels as compared with controls (GD9 $n = 5$, GD19 $n = 7$; $^{**}p < 0.001$). On average, pregnant dams consumed 1.69 ml/d (SEM = 0.0625) of 100% ethanol in a diluted solution. ***E***, Average gestational weight gain (g). EtOH-treated dams ($n = 10$) gained significantly less weight over the gestational period as compared with controls ($n = 10$; $^{*}p < 0.05$). ***F***, Average litter size. EtOH-treated dams ($n = 11$) delivered significantly smaller litters when compared with controls ($n = 10$; $^{*}p < 0.05$). Lower average EtOH-treated dam weight gain is related to decreased litter size and therefore not considered to be indicative of decreased caloric intake or malnutrition.

induced INC and gene expression phenotypes found in mouse neocortex on the day of birth may contribute to abnormal behavioral markers for anxiety and sensorimotor integration observed in PrEE mice 20 d later. As these are common phenotypes of children with FASD, we suggest that these PrEE-induced cortical defects may contribute to the cognitive-behavioral deficits observed in children with FASD.

Materials and Methods

Mouse colony. All breeding and experimental studies were conducted in strict accordance with protocol guidelines approved by the Institutional Animal Care and Use Committee at the University of California, Riverside. All mice were maintained in a CD1 background originally purchased from Charles River Laboratories. Female postnatal day (P)90 mice were paired with male breeders initially; the male was removed from the cage after conception, when the vaginal plug was confirmed [noon of the day of plug detection was staged at gestational day (GD) or embryonic day (E)0.5]. The average time to conception was 3 d with a range of 0–5 d. All timed pregnant female mice were subsequently housed individually, weight-matched and divided into two groups, experimental and control. For staging of pups, the day of birth was considered P0.

Dam ethanol administration. Experimental, ethanol-treated dams were provided an ethanol solution at noon on the day the vaginal plug was detected (GD 0.5) to the day of birth (GD 19.5). The 25% ethanol-in-water ethanol solution was provided *ad libitum* and self-administered by the dams, provided along with standard mouse chow, also *ad libitum*. Control dams were provided water and standard mouse chow *ad libitum*. Similar methods for generating a mouse model for FASD have been used previously (Galofré et al., 1987; Sbriccoli et al., 1999; Sari et al., 2001; Zhou et al., 2001; Powrozek and Zhou, 2005). The goal for this study was to demonstrate the impact of maternal ethanol consumption on murine offspring in an effort to understand mechanisms underlying FASD. We did not establish the treatment based on a specific human consumption model of FASD but instead created a moderate-high consumption model in mice.

Daily dam intake and gestational weight gain measurement techniques. Daily measurements of liquid and food intake were recorded at noon to assess potential confounding nutritional differences between experimental and control groups. A feeding bowl with 30 g standard mouse chow was provided to each pregnant dam on GD 0.5. This chow was reweighed daily at noon, and replenished to the 30 g start point. Average daily experimental values for food intake were computed from the 20 daily data values (GD 0.5–19.5) and compared with controls using *t* test analyses (Fig. 1*A*). Chow weights were measured using a standard Fisher Scientific scale. Average daily experimental values for liquid intake were computed from the 20 daily data values (GD 0.5–19.5) and compared with controls using *t* test analyses (Fig. 1*B*). Liquid (25% ethanol-in-water or water alone) intake was measured using a graduated drinking bottle. Each dam's body weight on GD 0.5 was subtracted from her body weight on GD19.5 and this value was recorded as maternal gestational weight gain. Dam body weight was measured using a standard Fisher Scientific scale. Gestational weight gain values of all experimental dams were compared with controls using *t* test analyses (Fig. 1*E*). Statistical significance for group differences among all dam measurements was set at $p < 0.05$.

Dam plasma osmolality measurement technique. Dam plasma osmolality was measured to rule out ethanol-induced dehydration, a potential confound in experimental dams. Whole blood samples taken from ethanol-exposed dams and control dams at GD 18.5 were added to ice-cold tubes and centrifuged at 4°C/1100 g for 10 min, obtaining a clear supernatant. Blood plasma osmolality was then measured using a Vapro 5520 vapor pressure osmometer (Wescor). Differences in plasma osmolality between ethanol-treated and control dams were computed using *t* test analyses (Fig. 1*C*). Statistical significance was set at $p < 0.05$.

Dam BEC measurement technique. Maternal blood ethanol content (BEC) resulting from self-administration of a 25% ethanol in water solution or water only was determined enzymatically. Blood samples were collected from ethanol-treated and control dams at two different gestational time points, mid-gestation (GD 9) and late-gestation (just before live birth, GD 19) between 0900 and 1200 h. Whole blood (0.2 ml) was collected and immediately mixed with 1.8 ml of 6.25% trichloroacetic acid and centrifuged at 2000 rpm for 2 min to obtain supernatant. The sample was then mixed with an alcohol reagent (A7504-39; Pointe Scientific) and assayed immediately using a Nanodrop ND-1000 Spectrophotometer at 340 nm wavelength. Blood ethanol standards were created by mixing alcohol standard (104 mg/dl) with alcohol reagent and immediately assayed. Each sample was analyzed in duplicate and experimental

Table 1. Number of cases (*n*) by experimental type

	Control	PrEE
Pregnant dams	32	36
Pup body wt	36	44
Pup brain wt	11	10
Pup cortical length	12	16
No. litters for anatomical/gene expression	20	21
Dye tracing: Anatomical (P0)	13 hemisects	11 hemisects
Gene expression: Molecular (P0)	7 hemisects	7 hemisects
Suok/Ledge tests: Behavioral (P20)	26 x-fost.	20 x-fost.

Number of adult female mice used for dam measures (Fig. 1). Number of pups used for body, brain weight, and cortical length assessments (Fig. 2). Number of litters used for anatomical and gene expression studies. Number of P0 mice used for dye tracing/anatomical studies (Figs. 3–7). Number of P0 mice used for gene expression/molecular studies (Figs. 8–Fig. 9). P20 mice used for behavioral studies (Figs. 10–11). x-fost., Number of cross fostered pups.

samples were compared with that of alcohol standard to determine blood ethanol concentrations. Pregnant nonethanol-treated dams were used as negative controls to insure proper assay analysis. Differences in BEC between ethanol-treated and control dams were computed using *t* test analyses (Fig. 1*D*). Statistical significance was set at $p < 0.05$.

Pup measurement techniques and tissue preparation. On the day of birth, experimental and control pup litter size was recorded and each pup was weighed individually using a Fisher Scale. Pups to be used in the newborn INC and gene expression studies were killed via hypothermia and transcardially perfused with 4% paraformaldehyde (PFA) in 0.1 M phosphate buffer, pH 7.4. The brains were immediately removed from the skull, weighed, measured for cortical length using a micrometer, hemisected, and postfixed in 4% PFA for 6 h. One hemisphere per brain was used for anatomical tracing, and the other was step-immersed and stored in methanol at −20°C for *in situ* hybridization (ISH). Brain tissue used for anatomical tracing and ISH was obtained from pups of 21 experimental and 20 control litters to capture natural variability. A subset of pups from each litter were moved to the cage of a control dam that had just given birth, after her control pups were removed. Control dams were needed to foster PrEE newborn pups postnatally as pup mortality was high with ethanol-treated dams. Twenty PrEE pups were fostered and housed with a control foster mother until age P20 when behavioral assays commenced. Twenty-six control pups used in behavioral experiments were also cross-fostered for 20 d with control dams to eliminate any confounds associated with cross-fostering (Table 1). Control and experimental pup measures of litter size, body, and brain weight, measured using a Fisher Scale, and cortical length, measured using a micrometer, were analyzed using *t* test analyses to assess group differences (Fig. 1*F*; Fig. 2). Statistical significance was set at $p < 0.05$.

Anatomical tracing techniques. To determine trajectories of INC development in the newborn mouse exposed prenatally to ethanol, single crystals of 1,1′-Dioctadecyl-3,3,3′,3′-tetramethylindocarbocyanine (DiI; Invitrogen) and 4-(4-(dihexadecylamino)styryl)-*N*-methylpyridinium iodide (DiA; Invitrogen) were placed in the developing sensory neocortex of one hemisphere. Dye crystals were placed in one of two locations using a coordinate grid for cross-case reliability: parietal lobe (putative somatosensory cortex) or occipital lobe (putative visual cortex). Because cortical length is decreased by ~10% in PrEE newborns, smaller crystals were placed into the PrEE cortices to account for the difference. The lengths of all crystals were measured using a micrometer and inserted into the cortex perpendicular to the layers to a depth where the tip of the crystal was just below the cortical surface. Methods for dye crystal placement have been described in detail previously (Huffman et al., 2004; Dye et al., 2011a,b, 2012). After dye placement, the hemispheres were immersed in 4% PFA and stored at room temperature for a period of 4–6 weeks to allow for transport of tracer; retrogradely labeled cells in dorsal thalamic nuclei were visually verified in the hemisphere before sectioning. Brain hemispheres were embedded in low-melting point agarose and sectioned in the coronal plane into 100 μm sections using a vibratome. Sections were stained with 4′, 6-diamidine-2-phenylindole dihydrochloride crystallized (DAPI; Roche), mounted onto glass slides, coverslipped with Vectashield mounting medium for fluorescence (Vector Laboratories), and digitally imaged (see Fig. 3). The size of dye placement locations (DPLs) and their associated spread were measured in the sections and recorded as a percentage of cortical length in each case. This analysis was done to ensure that the relative size of the DPL spread was consistent across control and experimental cases (see Fig. 6*A*,*C*). Differences in somatosensory and visual DPL sizes in experimental and control cortices were computed using *t* test analyses. Statistical significance was set at $p < 0.05$. The location of the dye placement was verified for each and every case using thalamocortical labeling observed in sections of experimental and control brain hemi-sections (see Fig. 5). Specifically, it was of paramount importance that the DPL for one sensory region (for example, somatosensory) did not spread into neighboring visual cortex during the time allowed for tracer transport. As had been done previously (Huffman et al., 2004) putative somatosensory cortex DPLs were included in our analysis if retrogradely labeled cells were observed in the ventral posterior (VP) nucleus of the dorsal thalamus and retrogradely labeled cells were absent from other sensory nuclei, such as the lateral geniculate (LG) nucleus of the dorsal thalamus. Putative visual cortex DPLs were included in our analysis if retrogradely labeled cells were observed in the LG and retrogradely labeled cells were absent from other sensory nuclei, such as the VP. In this study, we did not systematically analyze thalamocortical connections for a PrEE phenotype; we used these parallel sensory pathways to aid in the differentiation of our putative somatosensory and visual cortex dye placements. Both DAPI counterstain and Cresyl violet (Nissl) was used to identify nuclear boundaries in dorsal thalamic tissue.

Analysis of dye tracings. All experimental and control sections were digitally imaged with three different filters using a Zeiss Axio Imager Upright Microscope equipped with fluorescence, and captured using a digital high-resolution Zeiss Axio camera (HRm) coupled to a PC running Axiovision software (version 4.7). Three filters used were as follows: blue for DAPI counterstain, red for DiI, and green for DiA labeling (excitation wavelengths: blue, DAPI 359 nm; red, Cy 3 550 nm; green, GFP 470 nm; emission wavelengths: blue, DAPI 461 nm; red, Cy 3 570 nm; green, GFP 509 nm). The three images were merged and saved in high-resolution TIF format. For the analysis of potential effects of PrEE on INCs at P0, we matched sections from experimental and control brains using DAPI stained landmarks such as the anterior commissure, anatomical divisions of the basal ganglia and hippocampus, rostral pole of the superior colliculus and presented the experimental and control raw data in a series, side by side (see Fig. 3). To illustrate our findings, we created 2 d reconstructions of the DPLs and retrogradely labeled cells from the section data, morphed into a lateral view of the neocortex (see Fig. 4). This technique, resulting in a "flattened" neocortex, has been used previously to illustrate the position of INCs and DPLs in sensory and motor neocortex of mice from embryonic ages to adult (Huffman et al., 2004; Dye et al., 2011a shows detailed methods). This neocortical flattening method effectively demonstrates putative boundaries of neocortical motor and sensory regions/areas in very young mice (Dye et al., 2011a). To determine somatosensory and visual cortex projection zone size as a percentage of the whole cortex, distance to the most rostral and most caudal retrogradely labeled cells was measured using a micrometer for each dye injection (see Fig. 6) and calculated as a percentage of total cortical length. Analyzing projection zone size and DPL spread (described above) as a percentage of whole cortex controlled for group differences in cortical length. Differences in somatosensory and visual projection zone sizes in experimental and control cortices were computed using *t* test analyses. Statistical significance was set at $p < 0.05$.

Cell counting. Fluorescence microscopic images of control and experimental frontal cortex hemisections from P0 brains injected with DiI and DiA in the putative visual and somatosensory cortices were used for cell counts. Care was taken to ensure only stereotaxically identical sections were compared. Images were first converted to a binary format; the threshold was then adjusted allowing for the visualization of individual cells using ImageJ (NIH). Labeled cells within the cortex, intermediate zone, and upper subplate were then separated by electronically placing bins around each area. Cells were added to the bin in which 50% or more of the cell body was located, and then counted. The average number of retrogradely labeled cells within the cortical plate was presented (see Fig. 7), with between group differences calculated using *t* test analyses. Statistical significance was set at $p < 0.05$.

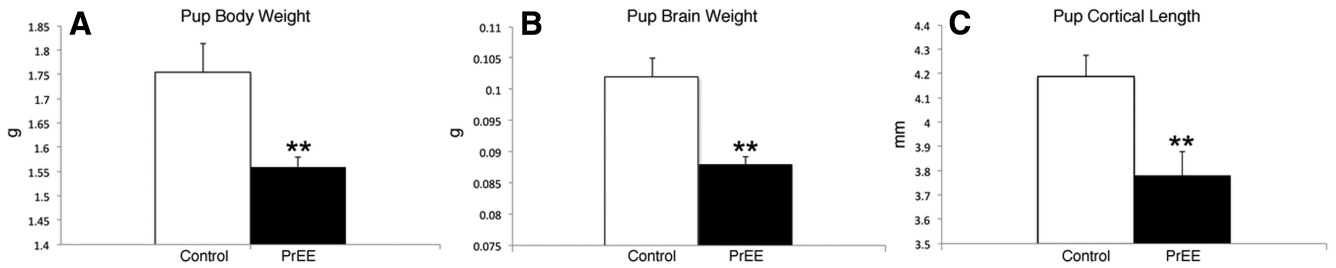

Figure 2. Average birth body weight, brain weight, and cortical length in PrEE and control newborn mice. ***A***, Average pup body weight (g). PrEE pups ($n = 44$) had significantly lower birth weights compared with controls ($n = 36$, $^{**}p < 0.001$). ***B***, Average pup brain weight (g). PrEE pups ($n = 10$) had significantly lower brain weights at birth compared with controls ($n = 11$, $^{**}p < 0.001$). ***C***, Average pup cortical length (mm). PrEE pups ($n = 16$) had significantly lower cortical lengths compared with controls ($n = 12$, $^{**}p < 0.001$).

Gene expression assays/analyses. Gene expression assays in PrEE and control brains were conducted using standard protocols and methods for nonradioactive free-floating *in situ* RNA hybridization (Shimamura et al., 1994; Garel et al., 2003; Huffman et al., 2004; Dye et al., 2011a,b). The following probes *RZRβ*, *Id2* (gifts from John Rubenstein, University of California, San Francisco, CA) and *Cadherin8* (*Cad8*, a gift from Masatoshi Takeichi, Riken Center for Developmental Biology, Japan) were used to identify patterns of neocortical gene expression in newborn mouse brain. To prepare tissue for *in situ* RNA hybridization, hemispheres reserved for hybridization (opposite hemispheres to those used in dye tracing studies) were embedded in gelatin-albumin and sectioned coronally at 100 μm using a vibratome. After hybridization, all sections were mounted in glycerol onto glass slides, coverslipped, and digitally imaged. Matched-level control and PrEE sections were presented together to show the altered expression patterns in PrEE cortex (see Fig. 8). These data were reconstructed in a coronal section where expression patterns of all three genes in typical control and PrEE cases were overlaid to aid in interpretation of the *in situ* hybridization data (see Fig. 8 *E1*,*E2*). Gene expression within specific, highlighted regions of neocortex of control and PrEE mice was analyzed (see Fig. 9). Transcript density was measured with ImageJ software and statistically analyzed to assess group differences. First, raw images were converted to a binary format and adjusted to a standardized threshold. A region of interest (ROI) was then electronically drawn over areas of either the rostral or the caudal parietal cortex. Transcript signal presence was then measured, and reported as area fraction of total ROI. This technique was recently described in detail by Dye et al. (2012).

Behavioral assays. In humans and nonhuman mammals, PrEE is associated with cognitive and behavioral deficits. To assess behavioral changes associated with prenatal ethanol exposure, we examined anxiety and sensorimotor integration function in adult PrEE mice through the use of two behavioral assays: the Suok test and the ledge test (see Fig. 10). These tests measure the animals' ability to integrate sensory inputs and motor outputs as well as anxiety (Wang et al., 2002; Wozniak et al., 2004; Kalueff et al., 2008; Glajch et al., 2012). The Souk apparatus was constructed in accordance with specifications published previously (Kalueff et al., 2008; see Fig. 11*A*). The apparatus consists of a smooth 2 m long aluminum rod, 3 cm in diameter, elevated to a height of 20 cm. The tube is separated into 10 cm segments by line markings and fixed to two clear acrylic end walls with a 20 cm virtual two-sector central zone around the placement point at the middle of the rod. Age P20 experimental PrEE and control mice were acclimated to the dimly lit behavioral room 1 h before testing. At the start of each 5 min testing period, animals were placed in the central zone with their snouts facing either end of the rod. Mice that fell off the rod were quickly repositioned on the apparatus in the same position and location. Several measures of behavior were observed and scored by trained researchers: (1) horizontal exploration activity, which included latency to leave the central zone and segments visited, (2) vertical exploration, which included the number of rears and wall leanings, (3) directed exploration as measured by side looks and head dips, (4) stereotyped grooming behavior proceeding uninterrupted in a cephalocaudal order, (5) risk assessment behaviors, indicated by stretch-attend postures, (6) vegetative responses, which included latency to defecate and number of defecations, and (7) sensorimotor ability, assessed by number of missteps and falls from the rod. Measures were recorded manually with stop-timers, with video recordings taken for backup. Following each trial, the apparatus was cleaned with 70% ethanol to remove olfactory cues. ANOVA with *post hoc* Student's *t* test was used to determine group differences on Suok measures (see Fig. 10*A–E*). Statistical significance was set at $p < 0.05$.

Immediately following the Suok test, animals were introduced to the ledge test apparatus (see Fig. 11 *B*, *C*). The apparatus consists of a vertically stabilized sheet of clear acrylic, 50 cm long and 30 cm high, with a thickness of 0.7 cm. Time to fall was then measured. If the animal was successful in traversing the ledge from one end to the other and back, or if the animal maintained balance for a full minute, the maximum score of 60 s was assigned. Following each trial, the apparatus was cleaned with 70% ethanol to remove olfactory cues. ANOVA with *post hoc* Student's *t* test was used to determine group differences on the ledge test (see Fig. 10*F*). Statistical significance was set at $p < 0.05$.

Results

Use of a novel mouse strain for FASD research

We mapped cortical gene expression and sensorimotor INC development in the neocortex of the CD1 mouse in detail from embryogenesis through adulthood (Dye et al., 2011a,b) and thus chose this murine strain for our FASD model. We demonstrate the efficacy of the model through multiple measures and have eliminated potential confounds (Fig. 1). As humans vary in their genotypes, it can be advantageous to expand research in the field by extending beyond models of one or two mouse lines.

Dam and pup measures

To rule out potential confounds of nutritional differences between groups, we monitored daily food and liquid intake as well as dam plasma osmolality, blood ethanol content, gestational weight gain, and litter size in both ethanol-treated and control groups. There were no significant differences between ethanol-treated and control dams in food intake (control 4.91 ± 0.17 g/d, PrEE 4.77 ± 0.20 g/d), liquid intake (control 6.27 ± 0.26 ml/d, PrEE 6.76 ± 0.25 ml/d), or plasma osmolality (control 311 ± 6 mosm/kg, PrEE 302 ± 8 mosm/kg; Fig. 1, *A–C*). On average, pregnant dams consumed 1.69 mls/d (SEM = 0.0625) of 100% ethanol daily administered in a diluted solution. To ensure consistent ethanol exposure, BEC was recorded at two time points during gestation in ethanol-treated and control dams. Ethanol-treated dams showed significantly higher BEC values compared with controls at both time points (Fig. 1*D*; GD 9 control 0.0 ± 0.0 mg/dl, GD 19 control 0.0 ± 0.0 mg/dl, GD 9 PrEE 103.57 ± 2.87 mg/dl, GD 19 PrEE 138.77 ± 3.13 mg/dl; $p < 0.001$). Gestational weight gain was significantly lower in ethanol-treated dams compared with controls (Fig. 1*E*; control 26.83 ± 2.08 g, PrEE 21.51 ± 1.32 g; $p < 0.05$); however, this effect correlates with a reduction in litter sizes among ethanol-treated dams (Fig. 1*F*;

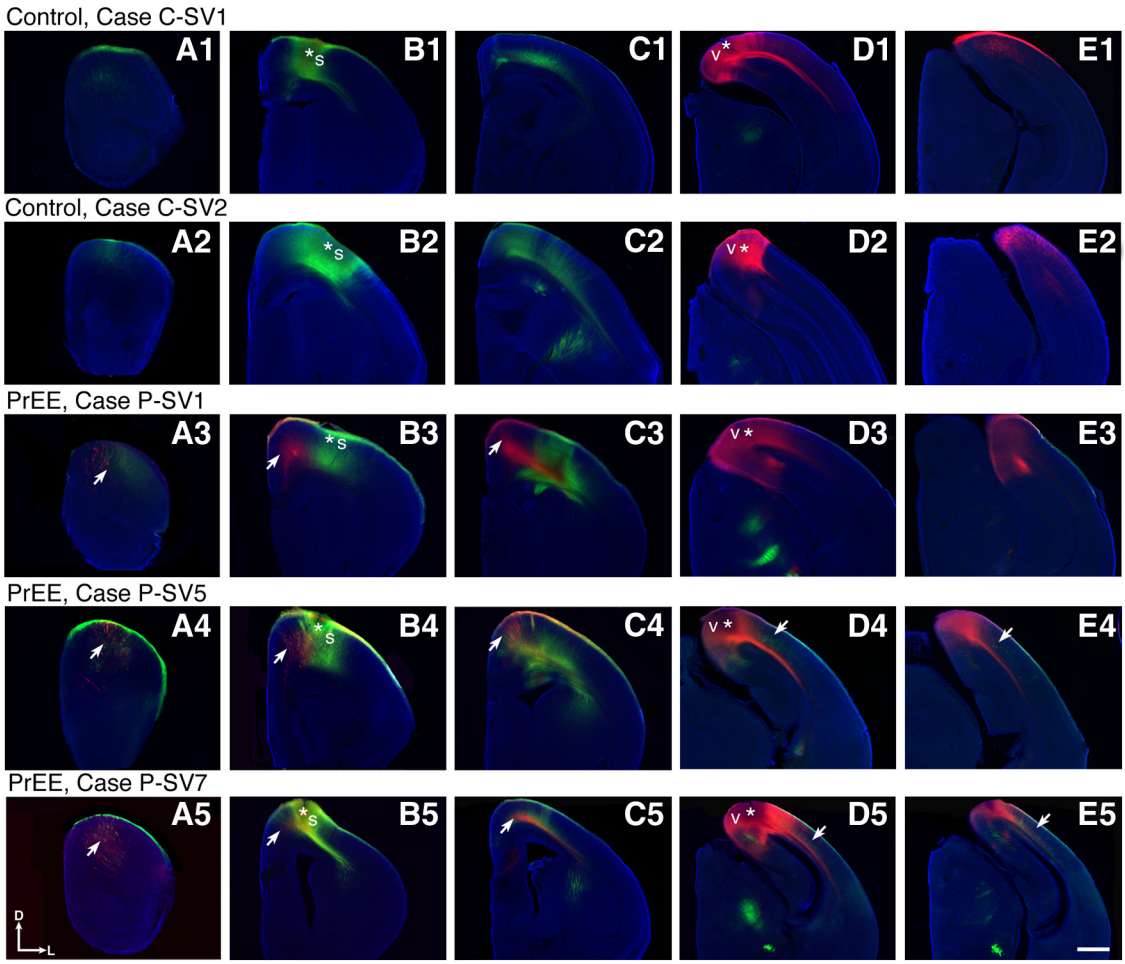

Figure 3. Somatosensory and visual INC development in control and PrEE brains at P0. Rostral to caudal series of 100 μm coronal sections of P0 hemispheres following DiA (green) or DiI (red) crystal placements in putative somatosensory (***B1***–***B5***, stars) and putative visual cortex (***D1***–***D5***, stars) of control and PrEE mouse brains. Sections were counterstained with DAPI. All arrows indicate retrogradely labeled cells. Far rostral, DiI labeled red cells from visual cortex dye placements are seen in frontal cortex of PrEE brains (***A3***–***A5***, red cells, arrows) and other rostral regions (***B3***–***B5***, ***C3***–***C5***) but not in controls (***A1***, ***A2***, ***B1***, ***B2***, ***C1***, ***C2***). DiA-labeled green cells from somatosensory cortex dye placements were seen in abnormally caudal locations in cortex of PrEE mice (***D4***, ***D5***, ***E4***, ***E5***) and not in corresponding locations in controls (***D1***, ***D2***, ***E1***, ***E2***). Raw images oriented dorsal (D) up and lateral (L) to the right. Scale bar, 500 μm.

control 11.7 ± 0.73 pups, PrEE 7.36 ± 0.97 pups; $p < 0.05$). In normal, untreated mice, reductions in litter size often result in higher pup weights; however, PrEE pups weighed significantly less than control newborns (Fig. 2*A*; control 1.75 ± 0.06 g, PrEE 1.56 ± 0.02 g; $p < 0.001$). Additionally, PrEE pup brain weights were significantly lower than brain weights of control pups, correlating with reduced body size (Fig. 2*B*; control 0.102 ± 0.003 g, PrEE 0.088 ± 0.001 g; $p < 0.001$). This was also correlated with a reduction in cortical length in the brains of PrEE pups; cortical lengths were significantly shorter, by ~10%, compared with controls (Fig. 2*C*; control 4.19 ± 0.09 mm, PrEE 3.78 ± 0.10 mm; $p < 0.001$).

Ipsilateral INCs in PrEE and control pups

A primary goal of this study was to characterize sensory INCs in newborn mice after prenatal ethanol exposure. Intraneocortical circuitry provides a foundation for complex sensorimotor integration in mammals and can be used to determine the boundaries of developing sensory and motor areas in the cortex of very young mice (Huffman et al., 2004; Dye et al., 2011a,b). Our data demonstrate that normal development of INCs was dramatically altered by prenatal ethanol exposure. Specifically, aberrant connections of the developing somatosensory and visual cortical areas are seen on the day of birth after prenatal ethanol exposure. In PrEE mice, retrogradely labeled cells from putative somatosensory cortex DPLs are observed in abnormally caudal positions within cortex (compare Fig. 3 *D1*,*D2* controls where no green cells are present with Fig. 3 *D4*,*D5* PrEE; arrows indicate ectopic green DiA label in PrEE cortex, with putative somatosensory DPLs starred in Fig. 3 *B1–B5*). These DiA labeled INCs in PrEE cortex are located in positions far caudal to controls in most PrEE cases.

DiI retrogradely labeled cells from putative visual cortex DPLs in control mice (Fig. 3 *D1*,*D2*, red DPLs starred) surround the DPL rostrally and caudally (Fig. 3*D1–E1*, *D2–E2*, red label in cortex), yet remain segregated from green cells labeled after a somatosensory DPL (Fig. 3*A1–C1*, *A2–C2*, green label in cortex). In PrEE newborn mice, however, DiI retrogradely labeled cells from putative visual cortex DPLs (Fig. 3*D3–D5*, red DPLs starred) are seen in far rostral locations (Fig. 3*A3–C3*, *A4–C4*, *A5–C5*, arrows highlight red label in rostral cortex). These labeled cell bodies projected their axons from an area within the frontal, motor cortex (Fig. 3*A3–A5*) and sensory-motor amalgam (Fig. 3*B3–B5*) to visual cortex, a projection pattern that does not exist in the normal mouse, at any age (Dye et al., 2011a,b). The phenotype of aberrant labeling of INCs resulting from putative so-

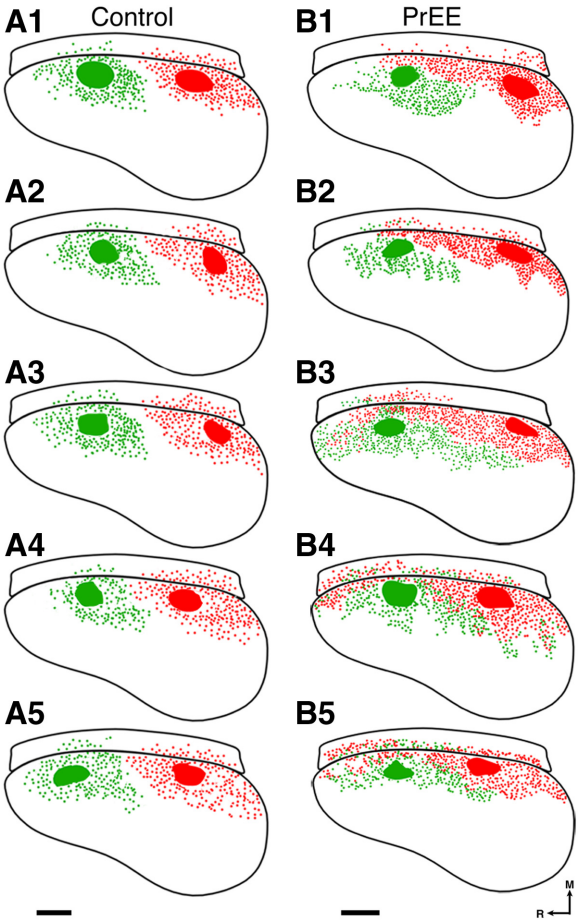

Figure 4. Flattened reconstructions of control and PrEE brains at P0. Flattened, lateral view reconstructions of single hemispheres of control (***A1–A5***) and PrEE (***B1–B5***) mouse brains. Dark lines = cortical outline; large red patches, DiI visual dye placements; large green patches, DiA somatosensory dye placements; small red and green dots, retrogradely labeled cell bodies. Reconstructions oriented medial (M) up and rostral (R) left. Scale bars, 500 μm.

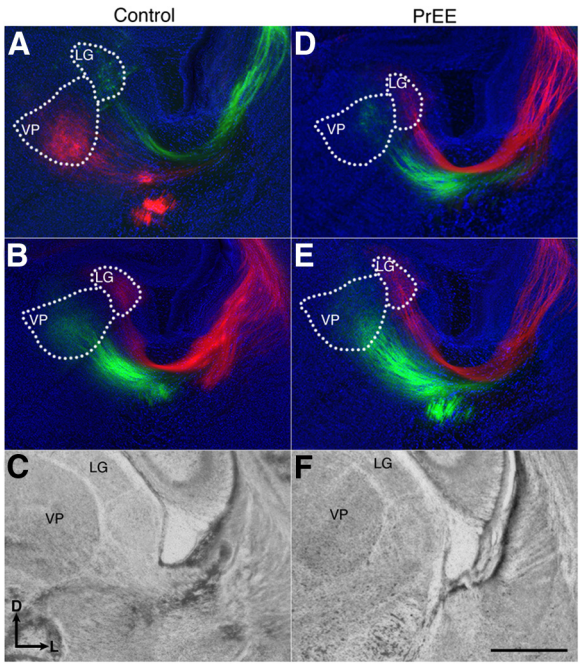

Figure 5. Retrograde thalamic nuclear labeling. High-magnification views of coronal 100 μm DAPI-stained DiI/DiA labeled hemisections and 40 μm Nissl-stained hemisections through the thalamus of representative cases of P0 control (***A–C***) and prenatal ethanol exposed, PrEE (***D–F***) brains. Retrograde labeling within the LGN and VP confirmed that DPLs were within visual and somatosensory cortices in all cases shown. Dye colors are reversed in ***A***; in that case DiA (green) was placed into putative visual cortex and DiI (red) was placed into putative somatosensory cortex. Dotted-lines in ***A***, ***B***, ***D***, ***E*** encircle discrete thalamic nuclei: VP and LG nucleus, also shown in Nissl sections in ***C*** and ***F***. Oriented with dorsal up and lateral to the right. Scale bar, 500 μm.

matosensory and visual cortex DPLs in brains of PrEE pups compared with control is illustrated in flattened lateral view reconstructions of five individual control cases and five individual PrEE cases (Fig. 4). Several cases are presented here to match DPL size and location and to show the variability in control and PrEE INC patterns. Control patterns of INCs vary to a small degree based in the exact position and size of the DPL; whereas PrEE cases have what appears to be more internal phenotypic variability (for example, although red labeling is seen in rostral locations after visual cortex DPLs in all cases, some cases, like Fig. 4*B1*,*B2* have milder phenotypes, whereas other cases, like *B3*,*B4* have more pronounced phenotypes). This variability in PrEE-related effects is consistent with literature in human models. Variability aside, as this figure demonstrates, the INC network is greatly disrupted in PrEE newborn mice. Although recently a multisensory area has been discovered in adult murine cortex (Olcese et al., 2013), there is no data to directly support the existence of this area in newborn cortex. As we have matched DPLs across many control and PrEE cases and only observed ectopic-labeled cells in PrEE cortices, we are confident our DPLs were within developing regions of somatosensory and visual cortex, rather than a multimodal region. All dye placements were verified as being within the borders of either putative somatosensory cortex or putative visual cortex via distinct retrograde labeling in either the VP or the LG of the dorsal thalamus, respectively (Fig. 5).

Despite similar DPL sizes across groups (Fig. 6*A*, somatosensory DPL size in control brains = 14.15 ± 0.01% and PrEE brains = 13.76 ± 0.06%, no significant difference; and Fig. 6*C*, visual DPL size in control brains = 14.45 ± 0.02% and PrEE brains = 14.46 ± 0.04%, no significant difference), the projection zones of retrogradely labeled cells from DPLs in putative somatosensory and visual cortex in PrEE mice, as a percentage of total cortical length, were determined to be substantially greater then that of controls (Fig. 6*B*, projection zones for somatosensory DPLs in control brains = 44.80 ± 4.96%, and PrEE brains = 65.38 ± 2.42%, $p < 0.05$; Fig. 6*D*, projection zones for visual DPLs in control brains = 41.36 ± 1.04%, and PrEE brains = 79.88 ± 7.64%, $p < 0.01$). This shows a breakdown in the specificity of INC position in sensory cortex.

Ectopically labeled cells from putative visual DPLs were observed in the frontal cortex of all PrEE pups (Fig. 7*B*), but not in controls (Fig. 7*A*). Cell counts of the frontal cortical area showed a dramatic increase of labeled cells in PrEE animals when compared with controls (Fig. 7*C*; control 0 ± 0 cells, PrEE 46.84 ± 12.26 cells; $p < 0.001$).

Gene expression

At P0, a handful of genes expressed within neocortex have been implicated in neocortical development as well as arealization, with graded or regional expression correlating with developing areal boundaries (Dye et al., 2011a). Included among these genes are *RZRβ*, *Cad8*, and *Id2*.

RZRβ *expression*

RZRβ is expressed in a high rostral to low caudo-lateral cortical gradient with some differential expression correlating with so-

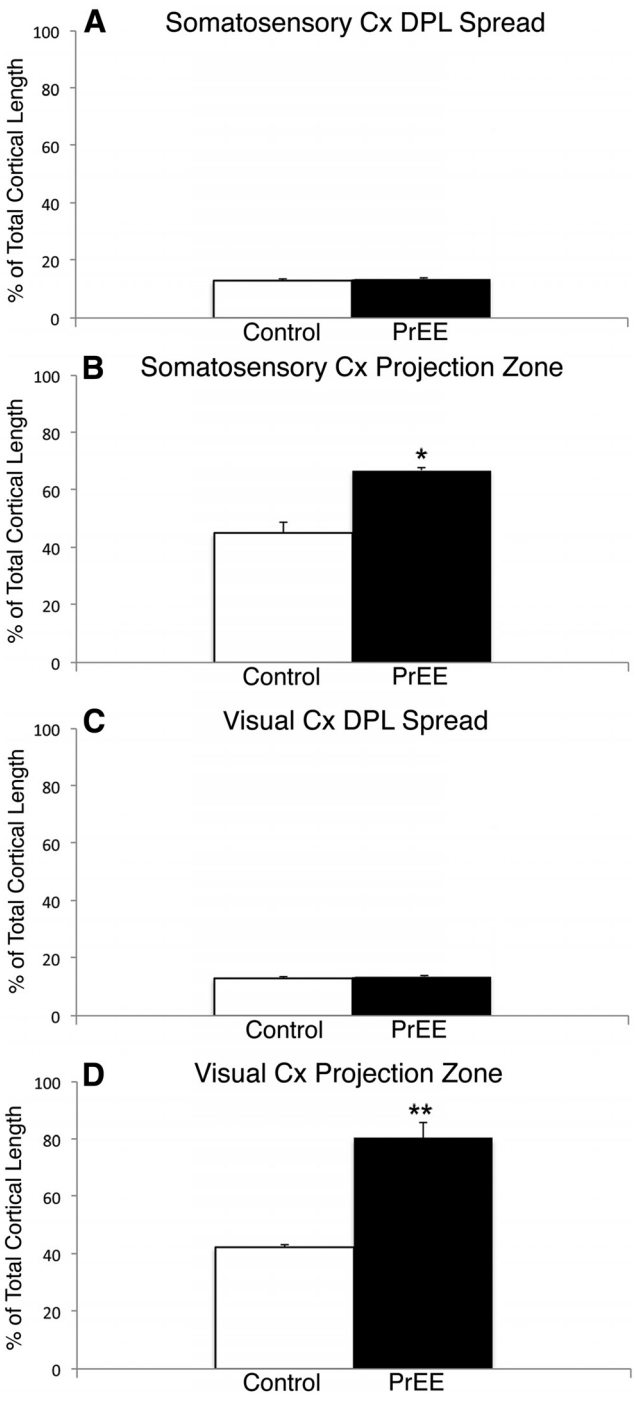

Figure 6. Average cortical DPL spread and projection zones in control and PrEE P0 brains. ***A***, Average spread of putative somatosensory cortex DPL. ***B***, Average projection zone of retrogradely labeled cells from putative somatosensory cortex DPLs. ***C***, Average spread of putative visual cortex DPL. ***D***, Average projection zone of retrogradely labeled cells from putative visual cortex DPLs. All PrEE brains showed no significant difference in DPL spread when compared with controls indicating no difference in dye injection size (***A***, ***C***). All PrEE brains had a significant increase in projection zone compared with controls indicating a lack of specificity of INC development in PrEE cortex (***B***, ***D***; $*p < 0.05$, $**p < 0.001$). DPL spread and projection zones of labeled cells were taken as a percentage of entire cortical length in all cases; PrEE $n = 9$, control $n = 8$.

matosensory cortical areas and marking the developing somatosensory/motor border in early postnatal mice (Dye et al., 2011a). In P0 control mice, an *RZRβ* expression gradient is observed in rostral sections (through caudal frontal cortex), with a noted absence in the most medial areas (Fig. 8*A1*, left arrow). In this same section, lateral expression is shown to be moderate (Fig. 8*A1*, right arrow). Rostral sections of parietal cortex show very light expression medially (Fig. 8*B1*, left black arrow) and moderate to strong expression along the lateral border of the cortex, where putative rostral somatosensory cortex is located (Fig. 8*B1*, black right arrow). Contrasting these findings, PrEE mice exhibit greater *RZRβ* expression in rostral-medial cortex (compare Fig. 8compare *A2*, PrEE left arrow with *A1*, control left arrow). Also, the lateral expression at this level is greater in PrEE brains compared with controls (Fig. 8compare *A2*, PrEE right arrow with *A1*, control right arrow). Additionally, a higher level of transcript in medial cortex is found in more caudal sections of the PrEE brain, in rostral parietal cortex (Fig. 8compare *B2*, PrEE left black arrow with *B1*, control left black arrow). The medial boundary of high *RZRβ* expression typically correlates with the developing medial border of somatosensory cortex in controls (Fig. 8 *B1*, white arrow; for review, see Dye et al., 2011a); this *RZRβ* boundary has shifted in PrEE neocortex (Fig. 8 compare *B1* and *B2*, white arrows) suggesting a disorganization of normal cortical patterning and development. The region of increased *RZRβ* expression located laterally in PrEE brains corresponds to somatosensory cortex and suggests a disruption of normal patterning (Fig. 8 compare *B2*, PrEE right black arrow with *B1*, control right black arrow). In normal mice, cells projecting to visual cortex at P0 are typically within *RZRβ*-positive zones, as *RZRβ* expression at this age corresponds with putative visual cortex and is anti-correlated with motor cortex (for review, see Dye et al., 2011a). In PrEE cortex, abnormal *RZRβ* expression near the boundaries of developing somatosensory and motor cortex correlated with an area that sends abnormal projections to the putative visual cortex in our dye tracing studies (Figs. 3, 4, 8). Atypical gene expression may generate the PrEE-related disruption in INC development, as the two processes have been linked in a previous report (Huffman et al., 2004). Quantification of *RZRβ* transcript density within regions of interest (in Fig. 9*A1*,*B1*, boxed ROI) revealed a significant increase in area fraction in PrEE mice in both rostral (Fig. 9 *A2*; control 9.09 ± 0.51%, PrEE 39.44 ± 0.32%, $p < 0.001$), and caudal (Fig. 9 *B2*; control 7.87 ± 0.24%, PrEE 46.01 ± 3.32%, $p < 0.01$) sections of the putative motor and somatosensory cortex.

Cad8 *expression*

Cad8 is strongly expressed in developing frontal, motor cortex in control mice (Dye et al., 2011a). Typically, regions of strong *RZRβ* and *Cad8* expression do not overlap in this neocortical region at P0. However, we found a lateral extension of *Cad8* expression in our PrEE cortices (compare Fig. 8*C1*,*C2*, arrows marking the lateral edge of *Cad8* expression). Patterns of *RZRβ* and *Cad8* expression at this level overlap slightly in the PrEE cortex compared with no overlap in the control (Fig. 8 *E1*,*E2*) demonstrating a disorganization of normal patterning. The shift in *Cad8* expression is also documented statistically in our density measures, showing increased transcript in our PrEE ROI in Figure 9*C1*, boxed (Fig. 9*C2*, control 45.15 ± 3.21%, PrEE 67.45 ± 2.00%; $p < 0.05$).

Id2 *expression*

In addition to abnormalities in *RZRβ* and *Cad8* expression, we found some differences in *Id2* expression in PrEE neocortex. In control P0 mice, developing cortical layers 3 and 4 are negative for *Id2* expression in rostro-medial cortex (Fig. 8*D1*, arrow). However, PrEE mice show an extension of the lateral *Id2*-positive

zones within these layers (Fig. 8*D2*, arrow). This can be seen relative to changes in *RZRβ* and *Cad8* expression in Figure 8*E2*. The PrEE-related *Id2-positive* zone (Fig. 8*D2*, arrow) is in a proximate location to the abnormal overlap of *RZRβ* and Cad8 (Fig. 8*E2*) and corresponds to a location of PrEE-induced ectopic dye labeling from a visual cortex DPL (Fig. 3). The shift in *Id2* expression is also documented statistically in our density measures, showing increased transcript in our PrEE ROI in Figure 9*D1*, boxed (Fig. 9*D2*, control 8.48 ± 0.82%, PrEE 40.19 ± 3.70%; $p < 0.001$).

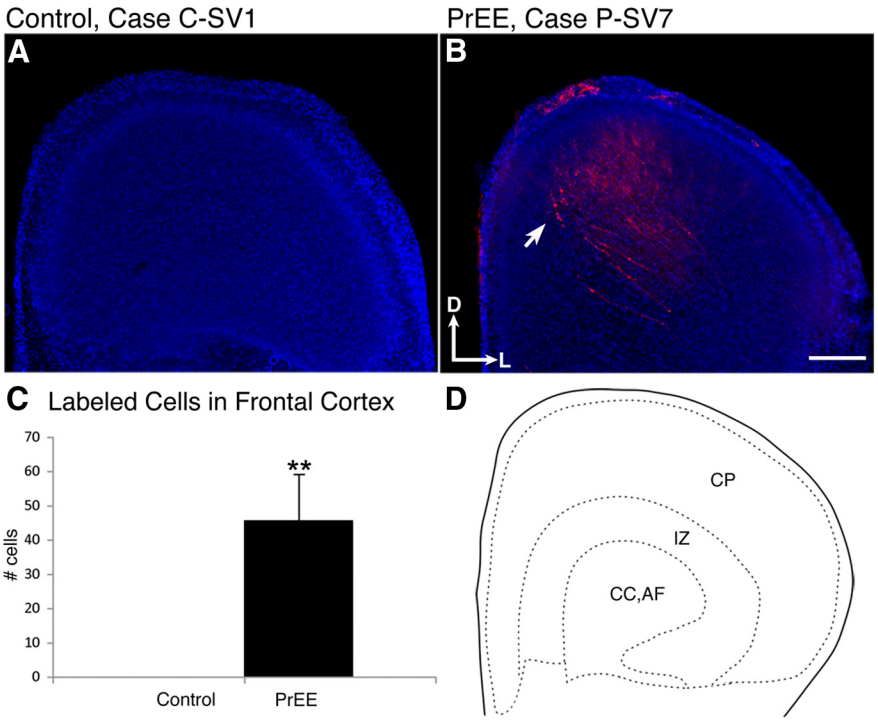

Figure 7. Analysis of frontal cortex INCs from visual cortex DPLs in control and PrEE *P0 brains*. ***A***, ***B***, DAPI stained coronal sections (100 μm) of P0 hemispheres following DiI DPL in putative visual cortex in a representative control (***A***) and prenatal ethanol exposed case (***B***). ***B***, Arrow indicates ectopic retrogradely labeled cells in frontal cortex. Dorsal (D) up and lateral (L) right. Scale bar, 500 μm. ***C***, Analysis of labeled cell counts in frontal cortex of control ($n = 7$) and PrEE brains ($n = 9$). PrEE brains showed significantly more labeled cells in frontal cortex (**$p < 0.001$). ***D***, Illustration of representative section. CP, Cortical plate; IZ, intermediate zone; CC,AF, corpus callosum, anterior forceps.

Behavioral assays

After documenting PrEE-related phenotypes in the neocortices of newborn mice, we began behavioral experiments in P20 control and PrEE mice to determine the behavioral readout of our perturbation. Data from these studies of anxiety and sensorimotor behavior revealed elevated anxiety, as well as deficits in balance and sensorimotor integration in mice exposed to ethanol *in utero*. The anxiogenic effect of PrEE manifested itself in a number of measures from the Suok test (see Fig. 11*A*). Stereotyped rearing/grooming events that progressed in the proper cephalo-caudal order in an uninterrupted "relaxed" manner, as opposed to rapid bursts of facial-only grooming, was scored for this test, revealing a decrease in PrEE animals compared with controls (Fig. 10*A*; control 1.72 ± 0.24, PrEE 0.94 ± 0.20, $p < 0.05$). This demonstrated increased anxiety in PrEE mice. PrEE mice also displayed significantly reduced directed exploration, indicative of elevated anxiety (Fig. 10*B*; control 70 ± 4.57, PrEE 51.88 ± 2.88, $p < 0.05$). Additionally, the latency, or time, to leave the central region of the Suok bar was significantly increased in PrEE mice when compared with controls, also characteristic of increased anxiety (Fig. 10*C*; control 3.75 ± 0.73 s, PrEE 6.83 ± 1.45 s, $p < 0.05$). Sensorimotor aptitude, assessed by the number of falls and missteps from the Suok apparatus, revealed significant deficits in PrEE subjects, which had significantly higher counts in each measure (Fig. 10*D*, falls; control 1.00 ± 0.35, PrEE 4.65 ± 0.81, $p < 0.01$; *E*, missteps; control 10.40 ± 3.88, PrEE 22.31 ± 1.93, $p < 0.01$). Motor activity in PrEE animals, as measured by segments crossed, did not differ statistically from controls due to high variability (control 83.50 ± 6.26, PrEE 98.53 ± 10.01; data not shown). In a final test of sensorimotor integration, the ledge test (Fig. 11*B*,*C*), PrEE mice demonstrated a reduced ability to maintain balance while traversing, or were immobile on the ledge when compared with control mice (Fig. 10*F*; control 60.00 ± 0.00, PrEE 49.14 ± 4.84, $p < 0.01$).

Discussion

Maternal consumption of alcohol (ethanol) while pregnant poses significant risk to the health of the offspring (Lundsberg et al., 1997; Windham et al., 1997; Maconochie et al., 2007; Aliyu et al., 2008; Strandberg-Larsen et al., 2008). PrEE induces cognitive-emotional deficits, behavioral disorders, motor dysfunction and developmental delays, implying disruption in neocortical function (Willford et al., 2006; Disney et al., 2008; Sayal et al., 2009; Lebel et al., 2012). Although inroads have been made to correlate abnormal brain development with human FASD phenotypes, the examination of intraneocortical connections in an animal model of FASD is novel. This report demonstrates the impact of PrEE on the development of this network and relates it to changes in cortical gene expression and behavioral dysfunction. As neocortical processes support human cognitive, motor, and behavioral abilities, it has been hypothesized that abnormal neocortical patterning and organization may underlie developmental dysfunction in humans (Lewis and González-Burgos, 2008; Benvenuto et al., 2009; Cherkasova and Hechtman, 2009).

PrEE impacts pup morphology

Adequate nutrition and hydration was maintained in our ethanol-treated dams, yet they birthed smaller litters containing smaller pups with smaller brains, an effect consistent with rat and human data (Abel, 1978; Streissguth et al., 1994; O'Leary-Moore et al., 2010). Although low birth-weight has been shown to delay development by slowing periphery-related thalamocortical patterning of the barrel field in early postnatal life (Hoerder-Suabedissen et al., 2008), we do not feel that decreased birth weight impacts our anatomical or molecular results as the pattern of INCs in PrEE newborn neocortex is truly ectopic and not found during embryogenesis.

Abnormal INC development in PrEE newborns

PrEE alters development of sensory intraneocortical connections. Visual and somatosensory INCs begin to delineate areal boundaries at E16.5, and continue to change until ~P3 where they maintain an adult-like form (Dye et al., 2011a,b). In normal development, retrogradely labeled cells from these dye placements do not overlap. In newborn PrEE mice, however, this seg-

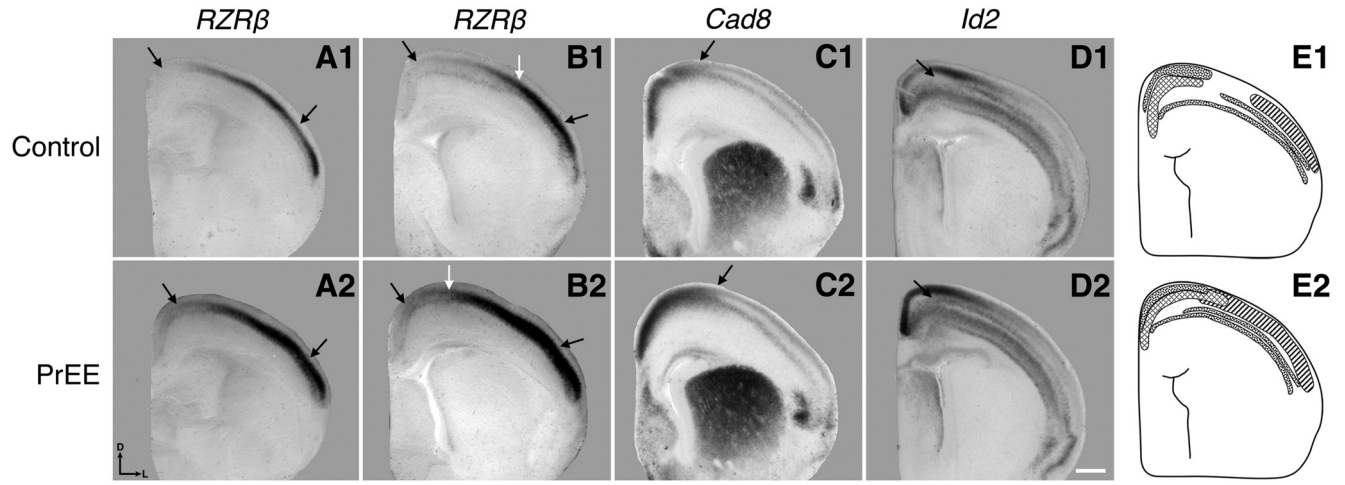

Figure 8. Neocortical expression of *RZRβ*, *Cad8*, and *Id2*. Coronal sections (100 μm) of P0 control and PrEE brain hemispheres following free-floating nonradioactive *in situ* hybridization with a probe against *RZRβ* (***A1***, ***A2***, ***B1***, ***B2***), *Cad8* (***C1***, ***C2***) or *Id2* (***D1***, ***D2***). ***A1***, Section through a caudal region of frontal cortex where left arrow denotes low medial cortical expression of *RZRβ* and a right arrow denotes moderate lateral expression in a control case. ***A2***, Section through a caudal region of frontal cortex where left arrow denotes moderate medial cortical expression of *RZRβ* and a right arrow denotes high lateral expression in a PrEE case. ***B1***, Section through a rostral region of parietal cortex where left black arrow denotes low medial cortical expression of RZRβ, a white middle arrow denotes the medial boundary of *RZRβ* expression, and a right arrow denotes moderate lateral expression of *RZRβ* in a control case. ***B2***, Section through a rostral region of parietal cortex where left black arrow denotes moderate medial cortical expression of *RZRβ*, a white middle arrow denotes the shifted medial boundary of *RZRβ* expression and a right arrow denotes high lateral expression of *RZRβ* in a PrEE case. ***C1***, Section through a rostral region of parietal cortex where black arrow denotes lateral boundary of *Cad8* expression in a control case. ***C2***, Section through a rostral region of parietal cortex where black arrow denotes a shifted lateral boundary of *Cad8* expression in a PrEE case. ***D1***, Section through a rostral region of parietal cortex where black arrow denotes an absence of *Id2* expression within cortical layers 3 and 4 in a control case. ***D2***, Section through a rostral region of parietal cortex where black arrow denotes an extension of the lateral *Id2* expression within layers 3/4. ***E1***, ***E2***, Patterns of gene expression compressed onto a coronal reconstruction of control (***E1***) or PrEE (***E2***) brains. Patterned areas represent gene expression as follows: *RZRβ*, diagonal line area; *Cad8*, crossed line area; *Id2*, dotted area. Dark line, cortical outline. Sections oriented dorsal (D) up and lateral (L) right.

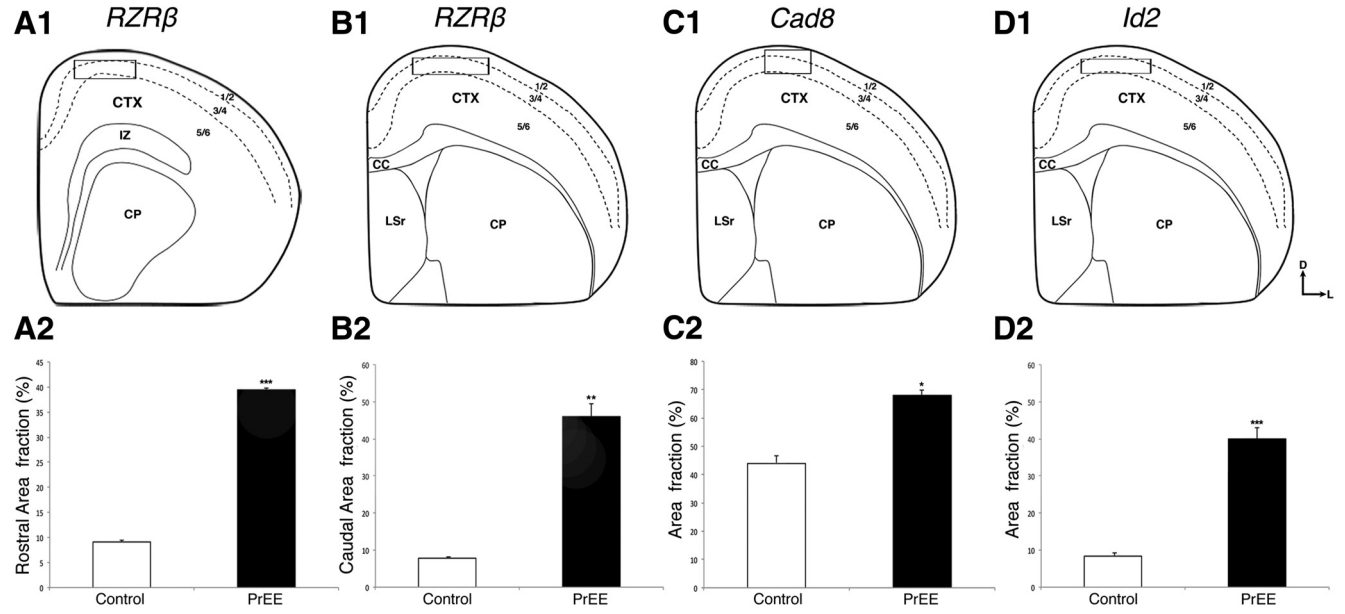

Figure 9. Analysis of neocortical expression of *RZRβ*, *Cad8*, and *Id2*. ***A1***–***D1***, Region of interest of quantified gene expression overlaid on representative coronal brain illustrations corresponding to graphs below. ***A2***–***D2***, Percentage area fraction of cells expressing *RZRβ* (***A2***, ***B2***), *Cad8* (***C2***), *Id2* (***D2***) within the ROI of caudofrontal cortex (***A2***) and rostral parietal cortex (***B2***–***D2***). A sharply increased percentage of transcripts are observed in PrEE cases when compared with control animals. CC, corpus callosum; CP, caudoputamen; CTX, cortex; LSr, lateral septal nucleus; Box, ROI. $*p < 0.05$, $**p < 0.01$, $***p < 0.001$.

regation of cells labeled from somatic and visual cortical area dye placements is disrupted and demonstrates a loss of modality specific organization without an overt change in thalamic input to these regions. These intraneocortical connections now overlap and appear disorganized, which could result in disorganized or atypical animal behavior.

The most pronounced INC phenotype in our PrEE model is the dramatic labeling of cells in frontal neocortex from dye placements in the putative visual area. This finding complements human PrEE data where changes in frontal cortical thickness were observed (Sowell et al., 2008), and frontal lobe damage in the adult human alcoholic brain was documented (Sullivan and Pfefferbaum, 2005). Frontal cortex regulates motor skill learning, decision-making, planning, judgment, attention, risk-taking, executive function, and sociality, processes greatly impacted by PrEE (Green, 2007; Xie et al., 2010; Zhou et al., 2011; Lebel et al.,

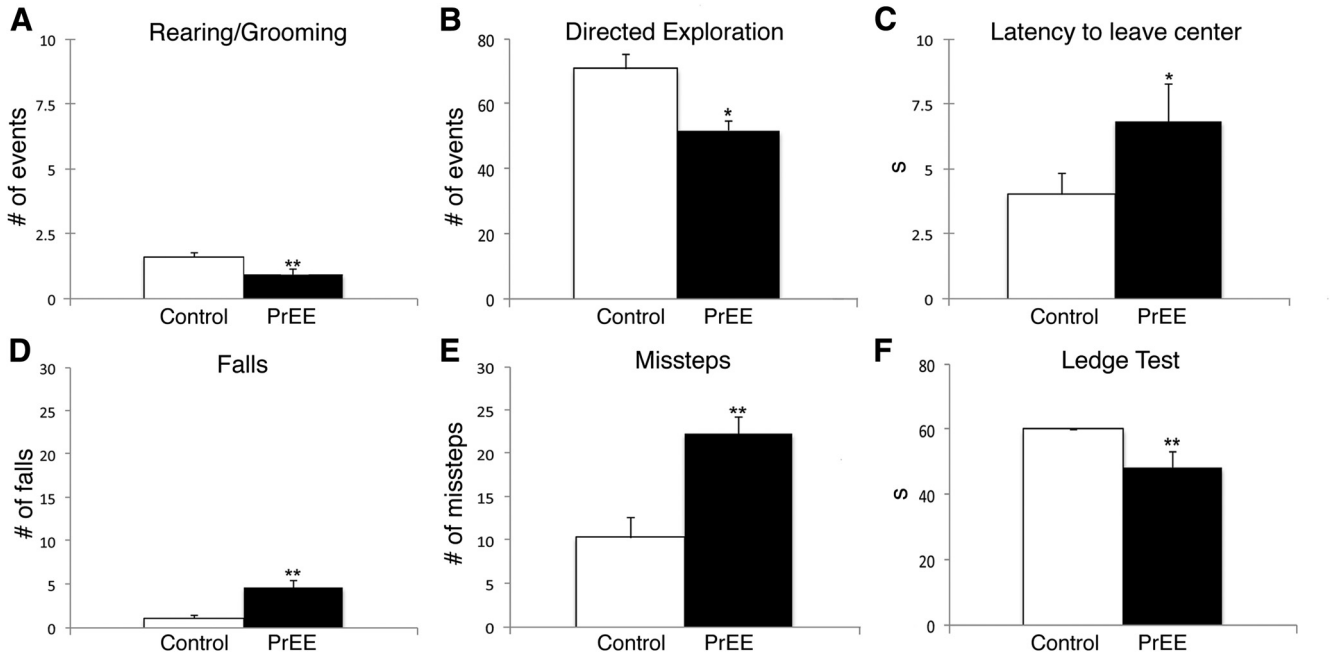

Figure 10. Behavioral measures in PrEE P20 mice. Significant group differences were found in measures of anxiety: ***A***, Stereotyped rearing/grooming (Suok test); ***B***, Directed Exploration (measured by side looks and head dips, Suok test); ***C***, Latency to leave center zone (center zone is the starting location for all control and PrEE mice, Suok test). In all three measures, PrEE mice ($n = 20$) showed increased anxiety compared with controls ($n = 26$). Significant group differences were also found in tests of motor coordination and sensorimotor integration: ***D***, Falls (Suok test); ***E***, Missteps (Suok test); ***F***, Ledge test. In all three measures, PrEE mice ($n = 20$) showed decreased motor coordination and sensorimotor integration compared with controls ($n = 26$); $^{*}p < 0.05$, $^{**}p < 0.01$.

2012). Frontal cortex cells in PrEE mice ectopically project to regions in visual cortex, possibly reflecting a defect in occipital patterning. PrEE-induced change in visual cortex function and visual attention task performance has been documented previously (Coles et al., 2002; Medina et al., 2003; Medina and Ramoa, 2005; Medina and Krahe, 2008).

Cells labeled from putative somatosensory area dye placements were found in ectopically caudal locations in PrEE mice. PrEE-induced disorganization of rodent somatosensory cortex has been demonstrated (Galofré et al., 1987; Rema and Ebner, 1999; Margret et al., 2005, 2006a,b; Powrozek and Zhou, 2005; Chappell et al., 2007; Oladehin et al., 2007), and abnormal cognitive-behavioral characteristics of FASD children are linked to parietal dysfunction, possibly reflecting abnormal connectivity as we describe (Lawrence et al., 2008; Sowell et al., 2008; Hamilton et al., 2010; for review, Schneider et al., 2011). Observation of a PrEE-induced disorganization in neuronal circuitry is novel and may underlie some aspects of sensorimotor, cognitive, and behavioral deficits observed in humans with FASD.

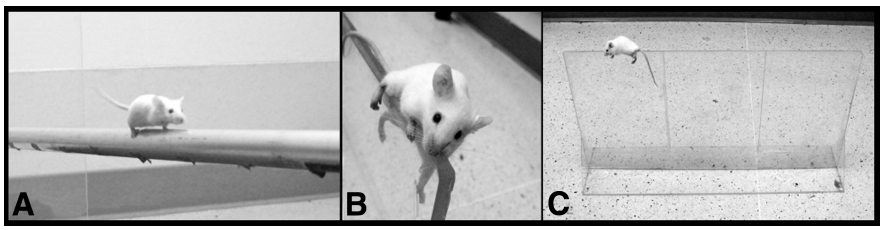

Figure 11. Behavioral tests in PrEE P20 mice. ***A***, Control mouse crossing the long elevated horizontal rod during testing on the Suok apparatus, to determine measures of anxiety (stereotyped rearing/grooming, directed exploration and latency to leave center portion of rod) as well motor coordination and sensorimotor integration (falls and missteps). ***B***, PrEE mouse struggling to maintain balance on ledge apparatus. ***C***, PrEE mouse traversing ledge apparatus during ledge test assay, exposing deficits in motor coordination of PrEE mice.

Potential mechanisms underlying the disorganized cortical circuitry in PrEE mice

The mechanisms responsible for abnormal developmental targeting of INCs in PrEE mice are unknown. One possibility lies with calcium channel function, which is known to impact axon growth and guidance cues. Altered calcium responses in growth cones have been observed after ethanol exposure, resulting in abnormal neuromorphogenesis associated with FASD (Mah et al., 2011). Calcium signal-related disruption in axon growth and/or guidance cues could impact targeting of intraneocortical axons leading to atypical development of cortical area borders and the physiological map (Margret et al., 2005, 2006a,b; Xie et al., 2010). This cascade of events could account for sensorimotor deficits observed in children with FASD (Franklin et al., 2008).

Although the mechanisms that establish cortical areas are not fully understood, gene expression, of a particular set of genes, has been implicated in border and areal specification (Miyashita-Lin et al., 1999; O'Leary and Nakagawa, 2002; Garel et al., 2003; Grove and Fukuchi-Shimogori, 2003; Huffman et al., 2004; Sur and Rubenstein, 2005; Cholfin and Rubenstein, 2008; Piñon et al., 2008; Dye et al., 2011a,b, 2012). Of these, *FGF8* has been shown to regulate the positioning of INCs across the cortical sheet by altering expression of other genes (Huffman et al., 2004). Specifically, a mutation in *FGF8* is correlated with changes in *RZRβ* and *Id2* expression, leading to ectopic targeting of INCs in early mouse development without a concomitant shift in thalamocortical afferents (Huffman et al., 2004). Thus, shifts in gene expression observed in PrEE mice may underlie the defect

in INC development. Although a positional shift in cortical gene expression in a PrEE mouse model is novel, research has shown that expression of *Pax6*, a transcription factor involved in neuronal developmental processes, is greatly reduced after PrEE (Aronne et al., 2008) and expression of a sufficiently large number of placental genes is altered (Rosenberg et al., 2010). PrEE leads to alterations in common signaling pathways and a reprogramming of genetic networks (Green, 2007). Additionally, genes expressed in neocortex were up- or down-regulated by PrEE when a combined transcriptome analysis of fetal human and mouse cortex was conducted (Hashimoto-Torii et al., 2011).

How might PrEE impact gene expression in the developing neocortex?

In this report, we document changes in expression patterns of *RZRβ*, *Cadherin8*, and *Id2* induced by prenatal ethanol exposure. Changes in gene expression reported in this study may be caused by altered DNA methylation, an epigenetic modification that cells use to mediate gene expression (Moore et al., 2013), cell differentiation, and embryonic development (Monk et al., 1987; Feng and Fan, 2009). Methylation occurs at the fifth position of cytosine and is driven by three conserved enzymes, DNA methyltransferase 1 (DNMT1), DNMT3A, and DNMT3B, which together are responsible for its deposition and maintenance, a function required for normal development (Li et al., 1992; Okano et al., 1999). Methyltransferase activity can be modified by exposure to ethanol; chronic exposure to ethanol is associated with reduced DNMT3B mRNA expression and hypermethylation in adults (Bönsch et al., 2006). Embryonic exposure to ethanol has been shown to alter DNA methylation patterns at neurulation, with increased methylation of genes on chromosome 10 and X correlating with an increase in neural tube defects (Liu et al., 2009). Furthermore, ethanol exposure impacts methyl donors (Mason and Choi, 2005), highlighting a possible mechanism by which ethanol, through methylation, can drive downstream epigenetic modifications and alter gene expression, as we have seen in this study (Haycock, 2009).

Abnormal behavior in P20 PrEE mice

Exposure to ethanol during critical periods of brain development can cause deficits in cognition and behavior even in the absence of gross morphological effects. These deficits may not become apparent until the child has begun the educational years (Streissguth et al., 1984; Conry, 1990; Streissguth et al., 1990; Streissguth and O'Malley, 2000; Kodituwakku, 2007). Humans with FASD and rodent models show deficits in sensory processing, social behaviors, motor learning and spatial functioning and often experience increased anxiety (Glavas et al., 2001; Kalberg et al., 2006; Hellemans et al., 2010,2010; Carr et al., 2010; Hamilton et al., 2010). In our study, prenatal exposure to ethanol produced changes in cortical gene expression and connectivity in newborn PrEE mice as well as poor sensorimotor function and increased anxiety at a later age. Specifically, P20 PrEE mice had difficulty with fine motor coordination tasks as measured by the Suok and Ledge tests. Increased anxiety observed in P20 PrEE mice replicates anxiety data in PrEE rat models (Cullen et al., 2013). Although we found atypical molecular and anatomical patterns in the neocortices of P0 PrEE mice and demonstrated a PrEE-related change in behavior at P20, these observations are, at this time, correlative. Until molecular and anatomical studies are conducted in the brains of P20 PrEE mice, caution must be taken in drawing causal relationships between the phenotypes.

In summary, prenatal ethanol exposure in mice produces biological phenotypes including reduced birth weight, brain weight, cortical length, and profound changes in neocortical gene expression, leading to abnormal development of intraneocortical circuitry. The precise development of the intraneocortical network is critical to cortical function, which, in turn is paramount for complex animal behavior. A defect in this network may underlie the disorganized cognitive and behavioral characteristics found in humans who suffer from FASD.

References

Abel EL (1978) Effects of ethanol on pregnant rats and their offspring. Psychopharmacology 57:5–11. CrossRef Medline

Aliyu MH, Wilson RE, Zoorob R, Chakrabarty S, Alio AP, Kirby RS, Salihu HM (2008) Alcohol consumption during pregnancy and the risk of early stillbirth among singletons. Alcohol 42:369–374. CrossRef Medline

Aronne MP, Evrard SG, Mirochnic S, Brusco A (2008) Prenatal ethanol exposure reduces the expression of the transcriptional factor Pax6 in the developing rat brain. Ann N Y Acad Sci 1139:478–498. CrossRef Medline

Bailey CD, Brien JF, Reynolds JN (2001) Chronic prenatal ethanol exposure increases GABA(A) receptor subunit protein expression in the adult guinea pig cerebral cortex. J Neurosci 21:4381–4389. Medline

Beckmann H (1999) Developmental malformations in cerebral structures of schizophrenic patients. Eur Arch Psychiatry Clin Neurosci 249:44–47. Medline

Benvenuto A, Moavero R, Alessandrelli R, Manzi B, Curatolo P (2009) Syndromic autism: causes and pathogenetic pathways. World J Pediatr 5:169–176. CrossRef Medline

Bönsch D, Lenz B, Fiszer R, Frieling H, Kornhuber J, Bleich S (2006) Lowered DNA methyltransferase (DNMT-3b) mRNA expression is associated with genomic DNA hypermethylation in patients with chronic alcoholism. J Neural Transm 113:1299–1304. CrossRef Medline

Carr JL, Agnihotri S, Keightley M (2010) Sensory processing and adaptive behavior deficits of children across the fetal alcohol spectrum disorder continuum. Alcohol Clin Exp Res 34:1022–1032. CrossRef Medline

Centers for Disease Control and Prevention (CDC) (2012) Alcohol use and binge drinking among women of childbearing age: United States, 2006–2010. MMWR Morb Mortal Wkly Rep 61:534–538. Medline

Chappell TD, Margret CP, Li CX, Waters RS (2007) Long-term effects of prenatal alcohol exposure on the size of the whisker representation in juvenile and adult rat barrel cortex. Alcohol 41:239–251. CrossRef Medline

Cherkasova MV, Hechtman L (2009) Neuroimaging in attention-deficit hyperactivity disorder: beyond the frontostriatal circuitry. Can J Psychiatry 54:651–664. Medline

Cholfin JA, Rubenstein JL (2008) Frontal cortex subdivision patterning is coordinately regulated by Fgf8, Fgf17, and Emx2. J Comp Neurol 509:144–155. CrossRef Medline

Coles CD, Platzman KA, Lynch ME, Freides D (2002) Auditory and visual sustained attention in adolescents prenatally exposed to alcohol. Alcohol Clin Exp Res 26:263–271. CrossRef Medline

Conry J (1990) Neuropsychological deficits in fetal alcohol syndrome and fetal alcohol effects. Alcohol Clin Exp Res 14:650–655. CrossRef Medline

Courchesne E, Redcay E, Morgan JT, Kennedy DP (2005) Autism at the beginning: microstructural and growth abnormalities underlying the cognitive and behavioral phenotype of autism. Dev Psychopathol 17:577–597. CrossRef Medline

Cullen CL, Burne TH, Lavidis NA, Moritz KM (2013) Low dose prenatal ethanol exposure induces anxiety-like behaviour and alters dendritic morphology in the basolateral amygdala of rat offspring. PLoS One 8:e54924. CrossRef Medline

Dawson G, Webb SJ, Wijsman E, Schellenberg G, Estes A, Munson J, Faja S (2005) Neurocognitive and electrophysiological evidence of altered face processing in parents of children with autism: implications for a model of abnormal development of social brain circuitry in autism. Dev Psychopathol 17:679–697. CrossRef Medline

Day NL, Helsel A, Sonon K, Goldschmidt L (2013) The association between prenatal alcohol exposure and behavior at 22 years of age. Alcohol Clin Exp Res 37:1171–1178. CrossRef Medline

Disney ER, Iacono W, McGue M, Tully E, Legrand L (2008) Strengthening the case: prenatal alcohol exposure is associated with increased risk for conduct disorder. Pediatrics 122:e1225–1230. CrossRef Medline

Dye CA, El Shawa H, Huffman KJ (2011a) A lifespan analysis of intraneocortical connections and gene expression in the mouse I. Cereb Cortex 21:1311–1330. CrossRef Medline

Dye CA, El Shawa H, Huffman KJ (2011b) A lifespan analysis of intraneocortical connections and gene expression in the mouse II. Cereb Cortex 21:1331–1350. CrossRef Medline

Dye CA, Abbott CW, Huffman KJ (2012) Bilateral enucleation alters gene expression and intraneocortical connections in the mouse. Neural Dev 7:5. CrossRef Medline

Feng J, Fan G (2009) The role of DNA methylation in the central nervous system and neuropsychiatric disorders. Int Rev Neurobiol 89:67–84. CrossRef Medline

Franklin L, Deitz J, Jirikowic T, Astley S (2008) Children with fetal alcohol spectrum disorders: problem behaviors and sensory processing. Am J Occup Ther 62:265–273. CrossRef Medline

Galofré E, Ferrer I, Fábregues I, López-Tejero D (1987) Effects of prenatal ethanol exposure on dendritic spines of layer V pyramidal neurons in the somatosensory cortex of the rat. J Neurol Sci 81:185–195. CrossRef Medline

Garel S, Huffman KJ, Martin G, Rubenstein JL (2003) Molecular regionalization of the neocortex is disrupted in Fgf8 hypomorphic mutants. Development 130:1903–1914. CrossRef Medline

Gillberg C (1999) Neurodevelopmental processes and psychological functioning in autism. Dev Psychopathol 11:567–587. CrossRef Medline

Glajch KE, Fleming SM, Surmeier DJ, Osten P (2012) Sensorimotor assessment of the unilateral 6-hydroxydopamine mouse model of Parkinson's disease. Behav Brain Res 230:309–316. CrossRef Medline

Glavas MM, Hofmann CE, Yu WK, Weinberg J (2001) Effects of prenatal ethanol exposure on hypothalamic-pituitary-adrenal regulation after adrenalectomy and corticosterone replacement. Alcohol Clin Exp Res 25: 890–897. CrossRef Medline

Green JH (2007) Fetal alcohol spectrum disorders: understanding the effects of prenatal alcohol exposure and supporting students. J Sch Health 77:103–108. CrossRef Medline

Grove EA, Fukuchi-Shimogori T (2003) Generating the cerebral cortical area map. Annu Rev Neurosci 26:355–380. CrossRef Medline

Hamilton DA, Akers KG, Rice JP, Johnson TE, Candelaria-Cook FT, Maes LI, Rosenberg M, Valenzuela CF, Savage DD (2010) Prenatal exposure to moderate levels of ethanol alters social behavior in adult rats: relationship to structural plasticity and immediate gene expression in the frontal cortex. Behav Brain Res 207:290–304. CrossRef Medline

Hashimoto-Torii K, Kawasawa YI, Kuhn A, Rakic P (2011) Combined transcriptome analysis of fetal human and mouse cerebral cortex exposed to alcohol. Proc Natl Acad Sci U S A 108:4212–4217. CrossRef Medline

Haycock PC (2009) Fetal alcohol spectrum disorders: the epigenetic perspective. Biol Reprod 81:607–617. CrossRef Medline

Hellemans KG, Sliwowska JH, Verma P, Weinberg J (2010) Prenatal alcohol exposure: fetal programming and later life vulnerability to stress, depression and anxiety disorders. Neurosci Biobehav Rev 34:791–807. CrossRef Medline

Hellemans KG, Verma P, Yoon E, Yu WK, Young AH, Weinberg J (2010) Prenatal alcohol exposure and chronic mild stress differentially alter depressive- and anxiety-like behaviors in male and female offspring. Alcohol Clin Exp Res 34:633–645. CrossRef Medline

Hoerder-Suabedissen A, Paulsen O, Molnár Z (2008) Thalamocortical maturation in mice is influenced by body weight. J Comp Neurol 511:415–420. CrossRef Medline

Hoffman EJ, Mintz CD, Wang S, McNickle DG, Salton SR, Benson DL (2008) Effects of ethanol on axon outgrowth and branching in developing rat cortical neurons. Neuroscience 157:556–565. CrossRef Medline

Hoyme HE, May PA, Kalberg WO, Kodituwakku P, Gossage JP, Trujillo PM, Buckley DG, Miller JH, Aragon AS, Khaole N, Viljoen DL, Jones KL, Robinson LK (2005) A practical clinical approach to diagnosis of fetal alcohol spectrum disorders: clarification of the 1996 institute of medicine criteria. Pediatrics 115:39–47. CrossRef Medline

Huffman KJ, Garel S, Rubenstein JL (2004) Fgf8 regulates the development of intraneocortical projections. J Neurosci 24:8917–8923. CrossRef Medline

Jacobson SW, Jacobson JL, Stanton ME, Meintjes EM, Molteno CD (2011) Biobehavioral markers of adverse effect in fetal alcohol spectrum disorders. Neuropsychol Rev 21:148–166. CrossRef Medline

Johansson M, Råstam M, Billstedt E, Danielsson S, Strömland K, Miller M, Gillberg C (2006) Autism spectrum disorders and underlying brain pathology in CHARGE association. Dev Med Child Neurol 48:40–50. CrossRef Medline

Jones KL, Hoyme HE, Robinson LK, Del Campo M, Manning MA, Prewitt LM, Chambers CD (2010) Fetal alcohol spectrum disorders: extending the range of structural defects. Am J Med Genet A 152A:2731–2735. CrossRef Medline

Kalberg WO, Provost B, Tollison SJ, Tabachnick BG, Robinson LK, Eugene Hoyme H, Trujillo PM, Buckley D, Aragon AS, May PA (2006) Comparison of motor delays in young children with fetal alcohol syndrome to those with prenatal alcohol exposure and with no prenatal alcohol exposure. Alcohol Clin Exp Res 30:2037–2045. CrossRef Medline

Kalueff AV, Keisala T, Minasyan A, Kumar SR, LaPorte JL, Murphy DL, Tuohimaa P (2008) The regular and light-dark Suok tests of anxiety and sensorimotor integration: utility for behavioral characterization in laboratory rodents. Nat Protoc 3:129–136. CrossRef Medline

Kelly YJ, Sacker A, Gray R, Kelly J, Wolke D, Head J, Quigley MA (2012) Light drinking during pregnancy: still no increased risk for socioemotional difficulties or cognitive deficits at 5 years of age? J Epidemiol Community Health 66:41–48. CrossRef Medline

Kelly Y, Sacker A, Gray R, Kelly J, Wolke D, Quigley MA (2009) Light drinking in pregnancy, a risk for behavioural problems and cognitive deficits at 3 years of age? Int J Epidemiol 38:129–140. CrossRef Medline

Kodituwakku PW (2007) Defining the behavioral phenotype in children with fetal alcohol spectrum disorders: a review. Neurosci Biobehav Rev 31:192–201. CrossRef Medline

Lawrence RC, Bonner CH, Newsom RJ, Kelly SJ (2008) Effects of alcohol exposure during development on play behavior and c-Fos expression in response to play behavior. Behav Brain Res 188:209–218. CrossRef Medline

Lebel C, Mattson SN, Riley EP, Jones KL, Adnams CM, May PA, Bookheimer SY, O'Connor MJ, Narr KL, Kan E, Abaryan Z, Sowell ER (2012) A longitudinal study of the long-term consequences of drinking during pregnancy: heavy *in utero* alcohol exposure disrupts the normal processes of brain development. J Neurosci 32:15243–15251. CrossRef Medline

Levitt P (1998) Prenatal effects of drugs of abuse on brain development. Drug Alcohol Depend 51:109–125. CrossRef Medline

Lewis DA, González-Burgos G (2008) Neuroplasticity of neocortical circuits in schizophrenia. Neuropsychopharmacology 33:141–165. CrossRef Medline

Li E, Bestor TH, Jaenisch R (1992) Targeted mutation of the DNA methyltransferase gene results in embryonic lethality. Cell 69:915–926. CrossRef Medline

Liu Y, Balaraman Y, Wang G, Nephew KP, Zhou FC (2009) Alcohol exposure alters DNA methylation profiles in mouse embryos at early neurulation. Epigenetics 4:500–511. CrossRef Medline

Livy DJ, Elberger AJ (2008) Alcohol exposure during the first two trimesters-equivalent alters the development of corpus callosum projection neurons in the rat. Alcohol 42:285–293. CrossRef Medline

Lundsberg LS, Bracken MB, Saftlas AF (1997) Low-to-moderate gestational alcohol use and intrauterine growth retardation, low birthweight, and preterm delivery. Ann Epidemiol 7:498–508. Medline

Maconochie N, Doyle P, Prior S, Simmons R (2007) Risk factors for first trimester miscarriage results from a UK-population-based case-control study. BJOG 114:170–186. CrossRef Medline

Mah SJ, Fleck MW, Lindsley TA (2011) Ethanol alters calcium signaling in axonal growth cones. Neuroscience 189:384–396. CrossRef Medline

Margret CP, Li CX, Elberger AJ, Matta SG, Chappell TD, Waters RS (2005) Prenatal alcohol exposure alters the size, but not the pattern, of the whisker representation in neonatal rat barrel cortex. Exp Brain Res 165:167–178. CrossRef Medline

Margret CP, Li CX, Chappell TD, Elberger AJ, Matta SG, Waters RS (2006a) Prenatal alcohol exposure delays the development of the cortical barrel field in neonatal rats. Exp Brain Res 172:1–13. CrossRef Medline

Margret CP, Chappell TD, Li CX, Jan TA, Matta SG, Elberger AJ, Waters RS (2006b) Prenatal alcohol exposure (PAE) reduces the size of the forepaw representation in forepaw barrel subfield (FBS) cortex in neonatal rats: relationship between periphery and central representation. Exp Brain Res 172:387–396. CrossRef Medline

Mason JB, Choi SW (2005) Effects of alcohol on folate metabolism: implications for carcinogenesis. Alcohol 35:235–241. CrossRef Medline

Medina AE, Krahe TE (2008) Neocortical plasticity deficits in fetal alcohol spectrum disorders: lessons from barrel and visual cortex. J Neurosci Res 86:256–263. CrossRef Medline

Medina AE, Ramoa AS (2005) Early alcohol exposure impairs ocular dominance plasticity throughout the critical period. Brain Res Dev Brain Res 157:107–111. CrossRef Medline

Medina AE, Krahe TE, Coppola DM, Ramoa AS (2003) Neonatal alcohol

exposure induces long-lasting impairment of visual cortical plasticity in ferrets. J Neurosci 23:10002–10012. Medline

Miyashita-Lin EM, Hevner R, Wassarman KM, Martinez S, Rubenstein JL (1999) Early neocortical regionalization in the absence of thalamic innervation. Science 285:906–909. CrossRef Medline

Monk M, Boubelik M, Lehnert S (1987) Temporal and regional changes in DNA methylation in the embryonic, extraembryonic and germ cell lineages during mouse embryo development. Development 99:371–382. Medline

Moore LD, Le T, Fan G (2013) DNA methylation and its basic function. Neuropsychopharmacology 38:23–38. CrossRef Medline

Okano M, Bell DW, Haber DA, Li E (1999) DNA methyltransferases Dnmt3a and Dnmt3b are essential for de novo methylation and mammalian development. Cell 99:247–257. CrossRef Medline

Oladehin A, Margret CP, Maier SE, Li CX, Jan TA, Chappell TD, Waters RS (2007) Early postnatal alcohol exposure reduced the size of vibrissal barrel field in rat somatosensory cortex (SI) but did not disrupt barrel field organization. Alcohol 41:253–261. CrossRef Medline

Olcese U, Iurilli G, Medini P (2013) Cellular and synaptic architecture of multisensory integration in the mouse neocortex. Neuron 79:579–593. CrossRef Medline

O'Leary DD, Nakagawa Y (2002) Patterning centers, regulatory genes and extrinsic mechanisms controlling arealization of the neocortex. Curr Opin Neurobiol 12:14–25. CrossRef Medline

O'Leary-Moore SK, Parnell SE, Godin EA, Dehart DB, Ament JJ, Khan AA, Johnson GA, Styner MA, Sulik KK (2010) Magnetic resonance microscopy-based analyses of the brains of normal and ethanol-exposed fetal mice. Birth Defects Res A Clin Mol Teratol 88:953–964. CrossRef Medline

Oster E (2013) Expecting better: why the conventional pregnancy wisdom is wrong and what you really need to know. New York: Penguin.

Pardo CA, Vargas DL, Zimmerman AW (2005) Immunity, neuroglia and neuroinflammation in autism. Int Rev Psychiatry 17:485–495. CrossRef Medline

Pelka GJ, Watson CM, Radziewic T, Hayward M, Lahooti H, Christodoulou J, Tam PP (2006) Mecp2 deficiency is associated with learning and cognitive deficits and altered gene activity in the hippocampal region of mice. Brain 129:887–898. CrossRef Medline

Piñon MC, Tuoc TC, Ashery-Padan R, Molnár Z, Stoykova A (2008) Altered molecular regionalization and normal thalamocortical connections in cortex-specific Pax6 knock-out mice. J Neurosci 28:8724–8734. CrossRef Medline

Powrozek TA, Zhou FC (2005) Effects of prenatal alcohol exposure on the development of the vibrissal somatosensory cortical barrel network. Brain Res Dev Brain Res 155:135–146. CrossRef Medline

Rema V, Ebner FF (1999) Effect of enriched environment rearing on impairments in cortical excitability and plasticity after prenatal alcohol exposure. J Neurosci 19:10993–11006. Medline

Robinson M, Oddy WH, McLean NJ, Jacoby P, Pennell CE, de Klerk NH, Zubrick SR, Stanley FJ, Newnham JP (2010) Low-moderate prenatal alcohol exposure and risk to child behavioural development: a prospective cohort study. BJOG 117:1139–1150. CrossRef Medline

Rosenberg MJ, Wolff CR, El-Emawy A, Staples MC, Perrone-Bizzozero NI, Savage DD (2010) Effects of moderate drinking during pregnancy on placental gene expression. Alcohol 44:673–690. CrossRef Medline

Santiago SE, Park GH, Huffman KJ (2013) Consumption habits of pregnant women and implications for developmental biology: a survey of predominantly Hispanic women in California. Nutr J 12:91. CrossRef Medline

Sari Y, Powrozek T, Zhou FC (2001) Alcohol deters the outgrowth of serotonergic neurons at midgestation. J Biomed Sci 8:119–125. CrossRef Medline

Sayal K, Heron J, Golding J, Alati R, Smith GD, Gray R, Emond A (2009) Binge pattern of alcohol consumption during pregnancy and childhood mental health outcomes: longitudinal population-based study. Pediatrics 123:e289–296. CrossRef Medline

Sbriccoli A, Carretta D, Santarelli M, Granato A, Minciacchi D (1999) An optimised procedure for prenatal ethanol exposure with determination of its effects on central nervous system connections. Brain Res Brain Res Protoc 3:264–269. CrossRef Medline

Schneider ML, Moore CF, Adkins MM (2011) The effects of prenatal alcohol exposure on behavior: rodent and primate studies. Neuropsychol Rev 21:186–203. CrossRef Medline

Shimamura K, Hirano S, McMahon AP, Takeichi M (1994) Wnt-1-dependent regulation of local E-cadherin and alpha N-catenin expression in the embryonic mouse brain. Development 120:2225–2234. Medline

Skogerbø Å, Kesmodel US, Wimberley T, Støvring H, Bertrand J, Landrø NI, Mortensen EL (2012) The effects of low to moderate alcohol consumption and binge drinking in early pregnancy on executive function in 5-year-old children. BJOG 119:1201–1210. CrossRef Medline

Sowell ER, Mattson SN, Kan E, Thompson PM, Riley EP, Toga AW (2008) Abnormal cortical thickness and brain-behavior correlation patterns in individuals with heavy prenatal alcohol exposure. Cereb Cortex 18:136–144. CrossRef Medline

Strandberg-Larsen K, Nielsen NR, Grønbeak M, Andersen PK, Olsen J, Andersen AM (2008) Binge drinking in pregnancy and risk of fetal death. Obstet Gynecol 111:602–609. CrossRef Medline

Streissguth AP, O'Malley K (2000) Neuropsychiatric implications and long-term consequences of fetal alcohol spectrum disorders. Semin Clin Neuropsychiatry 5:177–190. CrossRef Medline

Streissguth AP, Barr HM, Martin DC (1984) Alcohol exposure in utero and functional deficits in children during the first four years of life. Ciba Found Symp 105:176–196. Medline

Streissguth AP, Barr HM, Sampson PD (1990) Moderate prenatal alcohol exposure: effects on child IQ and learning problems at age 7 1/2 years. Alcohol Clin Exp Res 14:662–669. CrossRef Medline

Streissguth AP, Barr HM, Sampson PD, Bookstein FL (1994) Prenatal alcohol and offspring development: the first fourteen years. Drug Alcohol Depend 36:89–99. Medline

Sullivan EV, Pfefferbaum A (2005) Neurocircuitry in alcoholism: a substrate of disruption and repair. Psychopharmacology (Berl) 180:583–594. CrossRef Medline

Sur M, Rubenstein JL (2005) Patterning and plasticity of the cerebral cortex. Science 310:805–810. CrossRef Medline

Tochitani S, Sakata-Haga H, Fukui Y (2010) Embryonic exposure to ethanol disturbs regulation of mitotic spindle orientation via GABA(A) receptors in neural progenitors in ventricular zone of developing neocortex. Neurosci Lett 472:128–132. CrossRef Medline

Wang Q, Bardgett ME, Wong M, Wozniak DF, Lou J, McNeil BD, Chen C, Nardi A, Reid DC, Yamada K, Ornitz DM (2002) Ataxia and paroxysmal dyskinesia in mice lacking axonally transported FGF14. Neuron 35:25–38. CrossRef Medline

Waterman EH, Pruett D, Caughey AB (2013) Reducing fetal alcohol exposure in the United States. Obstet Gynecol Surv 68:367–378. CrossRef Medline

Willford J, Leech S, Day N (2006) Moderate prenatal alcohol exposure and cognitive status of children at age 10. Alcohol Clin Exp Res 30:1051–1059. CrossRef Medline

Windham GC, Von Behren J, Fenster L, Schaefer C, Swan SH (1997) Moderate maternal alcohol consumption and risk of spontaneous abortion. Epidemiology 8:509–514. CrossRef Medline

Wozniak DF, Hartman RE, Boyle MP, Vogt SK, Brooks AR, Tenkova T, Young C, Olney JW, Muglia LJ (2004) Apoptotic neurodegeneration induced by ethanol in neonatal mice is associated with profound learning/memory deficits in juveniles followed by progressive functional recovery in adults. Neurobiol Dis 17:403–414. CrossRef Medline

Xie N, Yang Q, Chappell TD, Li CX, Waters RS (2010) Prenatal alcohol exposure reduces the size of the forelimb representation in motor cortex in rat: an intracortical microstimulation (ICMS) mapping study. Alcohol 44:185–194. CrossRef Medline

Zhou D, Lebel C, Lepage C, Rasmussen C, Evans A, Wyper K, Pei J, Andrew G, Massey A, Massey D, Beaulieu C (2011) Developmental cortical thinning in fetal alcohol spectrum disorders. Neuroimage 58:16–25. CrossRef Medline

Zhou FC, Sari Y, Zhang JK, Goodlett CR, Li T (2001) Prenatal alcohol exposure retards the migration and development of serotonin neurons in fetal C57BL mice. Brain Res Dev Brain Res 126:147–155. CrossRef Medline

Zhou FC, Sari Y, Powrozek T, Goodlett CR, Li TK (2003) Moderate alcohol exposure compromises neural tube midline development in prenatal brain. Brain Res Dev Brain Res 144:43–55. CrossRef Medline

Zhou FC, Sari Y, Powrozek TA (2005) Fetal alcohol exposure reduces serotonin innervation and compromises development of the forebrain along the serotonergic pathway. Alcohol Clin Exp Res 29:141–149. CrossRef Medline

Zucca S, Valenzuela CF (2010) Low concentrations of alcohol inhibit BDNF-dependent GABAergic plasticity via L-type Ca^{2+} channel inhibition in developing CA3 hippocampal pyramidal neurons. J Neurosci 30:6776–6781. CrossRef Medline